Main individual and product characteristics influencing in-mouth flavour release during eating masticated food products with different textures: mechanistic modelling and experimental validation

Marion M. Doyennette, Isabelle Deleris Déléris, Gilles Feron, Elisabeth E. Guichard, Isabelle I. Souchon, Ioan-Cristian I.-C. Trelea

Main individual and product characteristics influencing in-mouth flavour release during eating masticated food products with different textures: mechanistic modelling and experimental validation

M. Doyennette[a, b], I. Déléris[a, b*], G. Féron[c, d, e], E. Guichard[c, d, e], I. Souchon[a, b], I. C. Tréléa[a,b]

[a]INRA, UMR 0782, F-78850 Thiverval Grignon, France. isabelle.deleris@grignon.inra.fr; isabelle.souchon@grignon.inra.fr

[b]AgroParisTech, UMR 0782, F-78850 Thiverval Grignon, France. cristian.trelea@agroparistech.fr

[c] INRA, UMR1324 Centre des Sciences du Goût et de l'Alimentation (CSGA), F-21000 Dijon, France. gilles.feron@dijon.inra.fr; elisabeth.guichard@dijon.inra.fr

[d] CNRS, UMR6265 CSGA, F-21000 Dijon, France

[e] Université de Bourgogne, UMR CSGA, F-21000 Dijon, France

Running title: Modelling release from masticated foods

[*]Correspondence to be sent to: Isabelle Déléris, UMR 0782, 78850 Thiverval Grignon, France, isabelle.deleris@grignon.inra.fr; tel: +33 (0)1 30 81 54 39; fax: +33 (0)1 30 81 55 97

Highlights:

- The developed model properly describes aroma release from masticated foods
- The mechanistic model includes both physiological and physical mechanisms.
- The most influent parameters for the intensity and the dynamics of the release were identified.
- The modelling approach highlighted aroma retention by lubricated mucosa.

Abstract

A mechanistic model predicting flavour release during oral processing of masticated foods was developed. The description of main physiological steps (product mastication and swallowing) and physical mechanisms (mass transfer, product breakdown and dissolution) occurring while eating allowed satisfactory simulation of *in vivo* release profiles of ethyl propanoate and 2-nonanone, measured by Atmospheric Pressure Chemical Ionization Mass Spectrometry on ten representative subjects during the consumption of four cheeses with different textures. Model sensitivity analysis showed that the main parameters affecting release intensity were the product dissolution rate in the mouth, the mass transfer coefficient in the bolus, the air-bolus contact area in the mouth and the respiratory frequency. Parameters furthermore affecting release dynamics were the mastication phase duration, the velopharynx opening and the rate of saliva incorporation into the bolus. Specific retention of 2-nonanone on mucosa was assumed to explain aroma release kinetics and confirmed when gaseous samples were consumed.

Keywords: dynamic model; aroma compounds; food oral processing; physiology; mass transfer

1. Introduction

The release of aroma compounds from food products during eating is a key step for their perception and ultimately for the acceptance of the product by the consumer. Food oral processing is complex [1] and flavour release induced by this processing depends on both the physiology and experience of subjects and on product properties. To identify what are these main properties explaining flavour release, it is necessary to develop an approach allowing the dissociation of mechanisms occurring during food oral processing. Mathematical modelling can help improving the understanding of the limiting mechanisms by pointing out the most important parameters related to the product and to the individual and allowing quantitative predictions of release dynamics. Therefore, models can help design the food products in a rational way, possibly targeted towards particular consumer groups such as young children, elderly or people with specific disorders.

The mechanistic modelling of aroma compound release during food consumption allows one to calculate, from known physical laws, the amount of aroma compounds transferred over time in each anatomical compartment involved during food oral processing (mouth, nasal cavity, pharynx).

The first mechanistic models have focused on predicting the release of aroma compounds from a two-phase emulsion (water, oil) in contact with gas [2]. They were based on physico-chemical principles governing the release of volatile molecules from a food matrix: (i) the mass conservation of volatile compound, (ii) the mass transfer at the emulsion-gas interface (interfacial penetration theory), (iii) equilibrium properties at the emulsion-gas interface [3]. First-order chemical kinetics have also been included in some models to describe reversible interactions between aroma compounds and non-volatile compounds such as macromolecules [2]. However, these first models are not really representative of *in vivo* phenomena because the geometry of the system (surfaces and volumes) is assumed constant (which is not the case

during food consumption) and they do not consider dynamic phenomena such as the dilution with salivary flow or the cyclic breathing of the subject. In addition, some of these models do not include any comparison with experimental data release [2].

Further development of these pioneering models has led to a better representation of *in vivo* conditions occurring during food consumption, by including notably parameters related to individual physiology, such as salivary flow, periodic breath, etc. [4, 5]. In addition, one of the major improvements in these models was to consider the aroma persistence phenomenon i.e. aroma release from bolus deposit covering the pharyngeal mucosa after swallowing. These models showed the relative roles of product and consumer characteristics and were validated against experimental data.

The first model including physiological data was proposed by Normand *et al*. [4] in the case of liquid products and highlighted two main release regimes: (i) release due to equilibrium batch extraction (only pertinent for few breaths after swallowing) and (ii) release from lubricated mucosa (persistence phenomena). In the case of semi-liquid food, the most comprehensive model to date is the one developed by Tréléa *et al*. [6] and further developed by Doyennette *et al*. [7] coupling aroma release in the mouth and in the pharynx.

Mechanistic models describing aroma release from masticated foods are far less available in the literature, mostly because of the difficulty to understand the complex mechanisms which are involved during the consumption of those foods. Compared to liquid products, mass transfer occurs through several interfaces (product/saliva, saliva/air) in “solid” matrices (needing mastication) [8, 9]. Also, additional phenomena have to be considered: product dissolution and melting due to intraoral manipulations (chewing, saliva incorporation, warming) and the generation of a dynamic exchange interface between product and saliva.

Existing models describing aroma release from solid food are not complete since they do not take breathing into account [5, 10]. Furthermore, the assumptions used are not always

transferable to other types of food matrices and to associated food oral processes than those studied (e.g. candy) or to other consumption patterns (e.g. sucking mechanism studied by Wright *et al*. [5]).

Hills and Harrison [10] also highlighted the importance of modelling the variation in the contact surface between the product and saliva, whose change in time plays a central role in the aroma compounds release. In their model, they suggest a multi-fragmentation theory to represent the chewing of a candy (assimilated to a cube). This approach provides a law of time change in the contact surface between product and saliva, using only two parameters: the number of bites and the duration of chewing. One might expect, however, that chewing real products, like cheeses for instance, will not always produce cubes and multiply the area by a factor of 2 after each bite. Other studies have also investigated the fragmentation of solids placed in the mouth under the action of chewing. The degree of fragmentation of a food can be determined by different types of experimental measurements such as the analysis of particle size distribution in the bolus [11]. These experimental data allow the determination of the laws of fragmentation depending on the type of food: deterministic analytic laws of product fragmentation over time [12], or probabilistic laws [8, 13-15]. While these approaches can be very comprehensive, they have several limitations. For example, some of them require complex experimental protocols that are difficult to implement (bolus spitting after a variable number of bites). Other approaches need the determination of many parameters (such as the number of chews, the number or the size of food particles after each chew, etc…), usually unknown, and which may depend on the product and/or on the individual.

From this literature review, it appears that modelling the release of aroma compounds during solid food consumption remains a challenging task and that the results of published studies are difficult to extrapolate to other experimental conditions. In this context, the present study proposes a model simulating the release of aroma compounds, applicable to different food

matrices and different individuals with a wide range of physiological characteristics. With this mechanistic model, our main objective was to understand the mechanisms and parameters governing the release of aroma compounds during the intra-oral manipulation and swallowing of “solid” food (needing chewing). To do so, simulations issued from the model were compared to *in vivo* release data of two aroma compounds, measured by atmospheric pressure chemical ionization mass spectrometry (APCI-MS) on ten panelists, during the consumption of four sorts of cheese, varying in composition and texture. Model assumptions are presented and their validity is discussed.

2. Mathematical modelling of *in vivo* aroma compound release

2.1.Principles of the model

The aroma release model described in this study applies to food products requiring mastication. It is an extension of the model developed for liquid and semi-liquid foods by Doyennette *et al*. [7]. The new insight is the consideration of the mastication process. The global eating process involves several steps shown in figure 1: the initial state of the system (product introduction in mouth), the intra-oral manipulation of the product, which consists in several masticatory cycles, one or more swallowing events and the resting phase (release during the post-mastication stage) which occurs when there is no more product in the mouth.

The intra-oral manipulation phase usually lasts until the first swallow. However, in some cases (particularly for firm products), it can extend beyond the first swallow.

Similarly to the model of Doyennette *et al*. [7], the present description of the swallowing step includes simultaneous contractions of the oral cavity and of the pharynx, leading to air and product expulsion, followed by relaxation and filling with fresh air. This will cause the expulsion of the bolus formed in the mouth into the pharynx. Each swallowing step leads to the deposit of a small part of the in-mouth liquid phase of the bolus on the pharyngeal walls.

A residual amount of the solid part of the bolus remains in the mouth and is chewed again and mixed with saliva in order to form a new food bolus suitable for swallowing.

A schematic representation of the four compartments involved in the model design, as well as their connections and the mechanisms responsible for flavour release, are given in figure 2. All variables and parameters of the interconnected compartments required for the model simulation are specified in this figure.

Compared to the previous model [7], two main differences can be observed: first, the presence of three instead of two sub-compartments in the mouth (the non-dissolved food product, which is the solid part of the bolus, the liquid phase of the bolus, made of saliva and dissolved food product and the air phase) and secondly, the opening of the velopharynx during chewing, allowing the transport of aroma compounds between the air phases of mouth and pharynx (figure 2).

Concerning the food bolus fragmentation under mastication, the particle size distribution in the bolus after each bite has already been described in literature [8, 11, 13-15]. However, these approaches require the knowledge of parameters such as food particle size after each chew, which is difficult to determine experimentally, particularly for pasty products like cheese used in the present study. The relevant parameter for aroma compound release is not the particle size itself, but the contact area between the solid and the liquid phase of the bolus. In this study, we focus on the generation of this area, as previously done in literature [16]. In the following paragraphs, the main differences with the previously published model for liquid products [7] are emphasized.

2.2.Mathematical description of mass transfer in mouth during the eating of masticated foods

The solid food product placed in the mouth is broken down during intra-oral manipulation. Two concurrent phenomena can occur:

• the transfer of aroma compounds from the non-dissolved product into the liquid phase of the bolus,

• the melting (dissolution) of the product in the liquid phase of the bolus due to the combined action of the mastication, the saliva incorporation and the warming of the product in the mouth. This also leads to the release of aroma compounds contained in the dissolved product towards the liquid phase of the bolus.

In practice, it is very difficult to distinguish between the relative contributions of each mechanism. Moreover, the phenomena of transfer and of dissolution can be described by very similar equations. Considering the studied products (cheeses), we arbitrarily chose to assign the release of aroma compounds into saliva to a single mechanism (dissolution) while being aware that the transfer also contributes to this process.

2.2.1. Air/bolus interfacial conditions in the oral cavity

Similarly to Doyennette *et al*. [7], the transfer resistance on the air side $1/k_{OA}$was assumed to be negligible when compared to the transfer resistance on the product side $1/k_{OL}$ (the orders of magnitude of the mass transfer coefficients, representing the reciprocal of the resistances, are 10^{-2} and 10^{-6} m/s respectively [17].

Therefore, the interfacial aroma compound concentration on the liquid bolus side, using the partition conditions at the interface, is given by:

$$C^*_{OAL}(t) = \frac{C_{OA}(t)}{K_{OAL}(t)} \quad (1)$$

The volatile mass flux between the air and the liquid bolus in the oral cavity ϕ_{OAL} is mainly determined by the resistance located on the bolus side and is given by the difference between the liquid bolus concentration (C_{OL}) and the interfacial concentration (C^*_{OAL}):

$$\phi_{OAL}(t) = k_{OL}(t) \times A_{OAL}(t) \times (C_{OL}(t) - C^*_{OAL}(t)) \quad (2)$$

2.2.2. Air in the oral cavity

In addition to the aroma compound flux from the liquid bolus, the air in the mouth can also exchange aroma compounds with the air in the pharynx. Jaw movements during mastication induce velopharynx opening and cyclic air flow between the pharynx and the mouth [18].

The variation of aroma concentration in the air in the oral cavity C_{OA} is thus due to the volatile flux from the liquid food bolus and from the air coming from the pharynx (Q_{OA}≥0 means that the air flows in the direction shown by the arrow in figure 2):

$$V_{OA}(t) \times \frac{dC_{OA}(t)}{dt} = \phi_{OAL}(t) + \begin{cases} Q_{OA}(t) \times (C_{FA}(t) - C_{OA}(t)) & if\ Q_{OA}(t) \geq 0 \\ 0 & if Q_{OA}(t) < 0 \end{cases} \quad (3)$$

Little is known on the real change in V_{OA}. It was assumed that the masticatory movements create a cyclic variation of the air volume V_{OA} around a mean value $V_{OA\,mean}$ as it has been observed by Matsuo *et al*. [18]. In this case:

$$V_{OA}(t) = V_{OA\,mean} + \Delta V_{OA} \times \sin(2 \times \pi \times fr_{opening} \times t) \quad (4)$$

Therefore, the air flow rate coming from the mouth Q_{OA} is calculated as follows:

$$Q_{OA}(t) = \frac{dV_{OA}(t)}{dt} = 2 \times \pi \times fr_{opening} \times \Delta V_{OA} \times \cos(2 \times \pi \times fr_{opening} \times t) \quad (5)$$

It is expected that ΔV_{OA}can be highly variable among individuals, but no quantitative data was found in the literature. A fair estimation of ΔV_{OA}seems to be 20% of $V_{OA\,mean}$, value which was used in our model. Based on observations from Matsuo *et al*. [18], we assumed that $fr_{opening}$ can vary among individuals, within a defined range. We supposed that the highest opening frequency was coordinated with the masticatory frequency ($fr_{masticatory}$), and that the lowest opening frequency was coordinated with the respiratory frequency (F_R). This assumption will be further discussed in the results and discussion section.

2.2.3. Product in the oral cavity

In line with the assumption of the dissolution rather than transfer mechanism discussed above, the aroma compound concentration in the solid (undissolved) food product fraction remains constant in time:

$$C_{OP}(t) = C_{OP}(0) \quad (6)$$

Due to dissolution and fragmentation processes, the volume of the solid food product decreases over time, while its contact area with the liquid phase of the bolus increases and then abruptly decreases due to swallowing.

The dissolution of the product at a rate *v* gives the following equation:

$$\frac{dV_{OP}(t)}{dt} = -v \times A_{OLP}(t) \quad (7)$$

Due to fragmentation induced by mastication, the contact area between the solid product present in the mouth and the liquid bolus increases in time. The exact rate of change of this contact area is not known for pasty products, like cheeses used in this study. In absence of more detailed information we assumed that, as long as some solid product is present in the mouth and a regular mastication behaviour were considered, its contact area with the liquid bolus evolves linearly over time. This simplifying hypothesis might be refined in the future based on more detailed studies, however. With this assumption:

$$\frac{dA_{OLP}(t)}{dt} = \begin{cases} \frac{A_{OLPdeg} - A_{OLPini}}{t_{deg} - t_0} & \textbf{if } V_{OP}(\boldsymbol{t}) > \mathbf{0} \\ 0 & \textbf{if } V_{OP}(\boldsymbol{t}) = \mathbf{0} \end{cases} \quad (8)$$

with the index "*deg*" meaning “at the current deglutition moment”, and the index "*ini*" meaning “at food product introduction in mouth” (at t_0) or “just after the previous deglutition”.

2.2.4. Liquid bolus in the oral cavity

The liquid bolus compartment has a composition which evolves over time. It is initially composed of pure saliva, and is progressively flavoured by the addition of dissolved product. Its volume increases with the addition of saliva (salivary flow) and with the incorporation of dissolved product, and periodically decreases after swallowing.

The volume of the bolus $V_{OL}(t)$ can be thus divided into two parts:

$$V_{OL}(t) = V_{OS}(t) + V_{OPD}(t) \quad (9)$$

In that case, we have:

$$\frac{dV_{OS}(t)}{dt} = Q_{OS} \quad (10)$$

with $\frac{dV_{OPD}(t)}{dt}$ the product dissolution rate, defined as

$$\frac{dV_{OPD}(t)}{dt} = v \times A_{OLP}(t) \quad (11)$$

The mass balance for a given aroma compound in the bolus leads to the following equation:

$$\frac{dV_{OL}(t) \times C_{OL}(t)}{dt} = \phi_{OLP}(t) - \phi_{OAL}(t) \quad (12)$$

with the volatile mass flux ϕ_{OLP} coming from product dissolution:

$$\phi_{OLP}(t) = v \times A_{OLP}(t) \times C_{OP}(t) \quad (13)$$

The mass flux ϕ_{OAL} is given by the difference between the aroma concentration in the liquid phase of the bolus (C_{OL}) and the interfacial concentration (C^*_{OAL}) (Eq. 2).

The properties of the liquid bolus relevant for aroma compound transfer, namely the air/bolus partition coefficient (K_{OAL}, Eq. 1) and the mass transfer coefficient (k_{OL}, Eq. 2) change with the relative fraction of the saliva and dissolved product in the liquid bolus. This dependence was previously established [19] and included in the model simulations.

2.3.Mathematical description of aroma release during the pharyngeal step

2.3.1. Bolus in the pharynx

Phenomena governing flavour release from the bolus in the pharynx are similar to the ones described for liquid products [7].

2.3.2. Air in the pharynx

The air in the pharynx exchanges aroma compounds with the bolus in the pharynx, and with the other compartments: the mouth (air flow $Q_{OA}(t)$), the nose (air flow $Q_{NA}(t)$) and the trachea (air flow $Q_{TA}(t)$). Compared to the model of Doyennette *et al.* [7], air flows to and from the mouth have been modified (due to the velopharynx opening during mastication). By

convention, the air flow rates indicated in figure 2 are positive if they follow the direction of the arrow. The air balance in the pharynx at any time gives the following relationship:

$$Q_{NA}(t) = -Q_{TA}(t) + Q_{OA}(t) \quad (14)$$

For the considered aroma compound, the mass balance in the air of the pharynx gives the equation:

$$V_{FA} \times \frac{dC_{FA}(t)}{dt} = \phi_{FAL}(t) + \begin{cases} -Q_{OA}(t) \times (C_{OA}(t) - C_{FA}(t)) & if\ Q_{OA}(t) < 0 \\ Q_{NA}(t) \times (C_{NA}(t) - C_{FA}(t)) & if\ Q_{NA}(t) \geq 0 \\ Q_{TA}(t) \times (C_{TA}(t) - C_{FA}(t)) & if\ Q_{TA}(t) \geq 0 \end{cases} \quad (15)$$

2.4.Conditions of the system after each deglutition

The deglutition step is very short compared to product residence time in mouth. It is thus described as quick contraction and relaxation events (figure 1).

2.4.1. Product and bolus in the oral cavity after deglutition

Aroma compound concentrations in the product and in the bolus are unchanged during deglutition. The volume of product in the oral cavity just after deglutition (V_{OPdeg+}) decreases and corresponds to the volume of product just before swallowing (V_{OPdeg-}) multiplied by the fraction of liquid bolus remaining in the mouth after deglutition (r_L), i.e. :

$$V_{OPdeg+} = V_{OPdeg-} \times r_L \quad (16)$$

Similarly, the liquid bolus/product contact area in the oral cavity after swallowing is calculated as:

$$A_{OLPdeg+} = A_{OLPdeg-} \times r_L \quad (17)$$

The volumes of saliva (V_{OSdeg+}) and of dissolved product ($V_{OPDdeg+}$) in the oral cavity decrease after swallowing. We assume that the bolus liquid part (saliva and dissolved product) is uniformly swallowed. Therefore, we have:

$$V_{OSdeg+} = V_{OSdeg-} \times \frac{V_{Salivadeg+}}{V_{OSdeg-} + V_{OPDdeg-}}, \text{ and } V_{OPDdeg+} = V_{OPDdeg-} \times \frac{V_{Salivadeg+}}{V_{OSdeg-} + V_{OPDdeg-}} \quad (18)$$

with $V_{Salivadeg+}$ being the volume of saliva usually present in the oral cavity after swallowing.

2.4.2. Aroma compound retention by lubricated mucosa

To take the reservoir effect of lubricated mucosa into account, additional compartments were included into the model. We assumed that air in the mouth, in the pharynx and in the nose was in contact with lubricated mucosa layers within the corresponding compartment. For example, in the nose, the volatile mass flux ϕ_{NAM} between the air and the mucosa is given by:

$$\phi_{NAM}(t) = k_{NM} \times A_{NAM} \times (C_{NM}(t) - \frac{C_{NA}(t)}{K_{NAM}}) \quad (19)$$

The mass balance of aroma compound in air contained in nasal cavity leads to:

$$V_{NA} \times \frac{dC_{FA}(t)}{dt} = \phi_{NAM}(t) + \begin{cases} Q_{NA}(t) \times (0 - C_{NA}(t)) & if\ Q_{NA}(t) \geq 0 \\ Q_{TA}(t) \times (C_{FA}(t) - C_{TA}(t)) & if\ Q_{TA}(t) \geq 0 \end{cases} \quad (20)$$

and in nasal mucosa:

$$V_{NM} \times \frac{dC_{NM}(t)}{dt} = -\phi_{NAM}(t) \quad (21)$$

Here, V_{NM} is the volume of lubricated mucosa which is involved in the interaction with the aroma compound. It can be expressed as

$$V_{NM} = e_{NM} \times A_{NAM} \quad (22)$$

Similar equations were added in the mouth and in the pharynx to take the effect of the lubricated mucosa present in these compartments into consideration. In the absence of more detailed information, the contact area between lubricated mucosa and air was arbitrarily set to half of the contact area between the bolus and the air in the mouth, as well as in the pharynx. Little information is available in the literature concerning values to be considered in the aroma retention model. The contact area between air and lubricated mucosa in the nose A_{NAM} was set to 160 cm² [20]. In literature, values comprised between 5.6×10^{-5} and 4.8×10^{-1} were mentioned for air/mucus partition coefficient of butanol and octanol in bullfrog [21]. Thus, a typical value of 1×10^{-3} was selected here. Concerning the mucosa layer thickness, Shojaei [22] gave values between 500 and 800 µm in mouth and 100 to 200 µm for the gingival mucosa. It is expected, however, that the aroma compound will not necessarily have time to

diffuse in the whole epithelium thickness, and these values are considered as upper limits for mucosa layer thickness involved in aroma retention.

3. Material and Methods

3.1. Flavoured cheese products

Four industrial cheese products (melt-cheese technology) varying in composition and texture (two fat levels and two firmness levels) and flavoured with ethyl propanoate and 2-nonanone were studied [23]. They were coded according to their characteristics, with a combination of letters as following: S or F for Soft or Firm respectively and l or h for low-fat or high-fat respectively.

Panelist selection and their physiological characterization at rest

Ten individuals were selected from a large panel composed of 44 subjects: they were verified to be representative of the whole panel (mean and standard deviation) concerning physiological data, masticatory behavior and APCI-MS release kinetics [23].

The volumes of oral, nasal and pharyngeal cavities of subjects were measured with the Eccovision Acoustic Rhinopharyngometer from Eccovision (Sleep Group Solutions, North Miami Beach, FL 33162). A software was developed to calculate automatically the air/product areas of oral and pharyngeal cavities for each individual [7].

The tidal volume of each individual was measured with a spirometer (Pulmo System II, MSR, Rungis, France) [23]. The respiratory frequency F_R used in the model was calculated directly from the acetone signal measured by APCI-MS.

3.2. In-nose measurements of aroma release by Atmospheric Pressure Chemical Ionization–Mass Spectrometry (APCI-MS) and data processing

Aroma release was measured using APCI-MS [23]. For each product, each panelist and for the three replicates, a mean curve and an envelope curve (representing the standard deviation of the replicates) were determined based on the peak lines (curve linking the maxima of

aroma release profile) [7]. Release kinetics were divided in two different phases: “phase 1” corresponded to the chewing phase before the first deglutition and “phase 2” corresponded to the rest of the chewing phase (if present) and to the resting phase. The end of phase 2 was set when less than 10% of the maximal intensity was reached. Areas under curve (AUC) were determined for each phase.

3.3. Physiological characterization of individuals during cheese consumption

Chewing activity, bolus saliva content and mouth coating were determined for each panelist as described in Repoux *et al*. [23].

It has been demonstrated from various studies [24, 25] that salivary flow during food consumption is much higher than the salivary flow at rest or artificially stimulated. Therefore, an average rate of saliva incorporation in the bolus during food product consumption (Q_{OS}) was estimated with the following equation:

$$Q_{OS} = \frac{percentage\ of\ incorporated\ saliva \times amount\ of\ food\ ingested}{100 \times duration\ of\ phase\ 1} \quad (23)$$

with the amount of food ingested = 6g, and phase 1 being the chewing phase before the first swallow. The percentage of incorporated saliva (relative to the product) was calculated as follows, based on moisture content of the initial cheese and of the bolus:

$$percentage\ of\ incorporated\ saliva = \frac{HM_{bolus}}{100 - HM_{bolus}} \times (100 - HM_{cheese}) - HM_{cheese} \quad (24)$$

The percentage of incorporated saliva and the duration of phase 1 were determined during two separate experimental sessions, which can induce biased calculation (the salivary flow rate is known to vary daily and with the physiological state of the individual). Therefore, the average rate of saliva incorporation in the bolus during food consumption calculated with Eq. 23 was only indicative and we preferred to use this parameter as a degree of freedom of the model for simulations.

In this study, neither the frequency nor the displacement amplitude of the soft palate during food consumption could be experimentally measured in a non-invasive way. Due to the

uncertainty on the actual values of these parameters and to the fact that they have a similar effect on the air flow rate (Eq. 5), the volume variation of the oral cavity during the consumption of cheese was arbitrarily fixed to a reference value of 20% of the mean volume and the opening frequency of the velopharynx was a degree of freedom of the model.

The contact area between the liquid bolus and the product just before swallowing ($A_{OLPdeglu}$) was calculated with the assumption of spherical particles:

$$A_{OLPdeglu} = \frac{3 \times V_{OPini}}{R} \quad (25)$$

The particle radius R was estimated with a compression device designed by the Laboratoire de Rhéologie (Grenoble, FRANCE) [26].

3.4. Air/bolus partition and mass transfer coefficients of aroma compounds in cheese bolus

The modification of the air/bolus partition coefficients of ethyl propanoate and 2-nonanone, due to modification of the bolus composition, was determined by the static phase ratio variation method (PRV) [27]. The mass transfer coefficients of aroma compounds into the bolus were obtained by non-linear regression from dynamic headspace experiments performed with Proton Transfer Reaction-Mass Spectrometry (PTR-MS) [7]. From those *in vitro* measurements, the relationships describing the modifications of air/bolus partition and the mass transfer coefficients of ethyl propanoate and 2-nonanone in bolus as a function of cheese/saliva mass ratio were integrated into the model. The cheese/saliva mass ratio r_{cs} used in the equations is given by:

$$r_{cs} = \frac{V_{OPD}}{V_{OPD} + V_{OS}} \quad (26)$$

3.5. Estimation of cheese dissolution rate in artificial saliva

Considering the previously mentioned assumption of product dissolution, the dissolution rate was estimated from measurements of the release of ionic species into warm artificial saliva, using a conductivity probe. This measurement was chosen for its simplicity and for the possibility to perform on-line measurements. The release of salts is considered here as a

marker of the matrix dissolution. The conductivity probe was calibrated at 35°C, with aqueous NaCl solutions prepared with deionised water. Concentrations were measured in g/L NaCl equivalent. A 6g-cylinder of cheese matrix, cut with a 24-mm punch, was placed in a beaker containing 400 ml of artificial saliva (including 0.216 g of mucin (from porcine stomach type II, SIGMA-ALDRICH) per 100g) and a magnetic stirrer. The monitoring of salt release (actually all species contributing to the conductivity signal) was made during two minutes using a conductivity meter (MPC HEITOLAB 350) and a probe (DCP 4). Product dissolution rate was determined by nonlinear regression using Matlab 7 (Natick, MA), using Eq. 27.

$$\phi_{salt}(t) = v \times A(t) \times (C_{P_{salt}} - C_{S_{salt}}\ \ (t)) \quad (27)$$

where ϕ_{salt} is the salt mass flux between the product and saliva, A(t) the product/saliva contact area and C_{Psalt} and C_{Ssalt} the salt concentrations in the solid product and in artificial saliva respectively.

3.6. Measurements of aroma compound retention by lubricated mucosa using Proton Transfer Reaction-Mass Spectrometry (PTR-MS)

Flavoured solutions were prepared with mineral water (Evian), ethyl propanoate and 2-nonanone (final concentration of 4.8mg/L for each). 134.8cm^3 Schott vials, equipped with caps fitted with two valves (Interchim SCAT or InterchimOmnifit, England), were half-filled with flavoured solutions and left at 35°C for 2 h to allow thermal equilibrium.

Five panelists were recruited for this specific measurement and were instructed to suck up a mouthful of vial headspace with a straw, to swallow it and to continue to breathe normally through the nose. A minimum of three replicates was performed for each individual. During this experiment, the dynamic release of aroma compounds was measured online using Proton Transfer Reaction Mass Spectrometry (PTR-MS, Ionicon Analytik, Innsbruck, Austria). The PTR-MS inlet was connected to the subject's nose *via* a 1/16" PEEK tube maintained at 60°C.

Air was sampled from the subject's nose at a flow rate of 35 cm^3/min *via* two inlets of a stainless nosepiece placed in both of the assessor's nostrils. The PTR-MS instrument drift tube was thermally controlled (T_{drift}=60°C) and operated at P_{drift}=200 Pa with a voltage set of U_{drift}=600 V. Measurements were performed with the multiple ion detection mode on specific masses with a dwell time per mass of 50 ms. Ethyl propanoate and 2-nonanone were respectively monitored at *m/z* 103 (molecular ion) and *m/z* 143 (molecular ion). In addition, *m/z* 59 (acetone) was monitored as a breath marker and *m/z* 21 (signal for $H_3{}^{18}O^+$) and *m/z* 37 (signal for water clusters H_2O-H_3O^+) were monitored to check the instrument performances and cluster ion formation.

3.7. Statistical analysis

Due to the small size and the non-normal characteristic of the dataset, classical analysis of variance was not appropriate (univariate procedure using SAS/Stat® software). Instead, Friedman tests were performed with an Excel program (available at www.Anastats.fr). Rankings of samples were then obtained by the non-parametric test of multiple comparisons (Bonferroni method, level of significance set at 5%). For the correlation test, the Spearman test was performed, with a level of significance set at 5% (www.Anastats.fr).

4. Results and Discussion

4.1. Model simulations: insights in non-measured variables and assumptions on governing mechanisms

Figure 3 shows the time variation of 9 out of the 15 model variables for the release of ethyl propanoate during consumption of the cheese matrix FFl. Values of physiological parameters were fixed to the panel mean.

The volume of product present in the mouth V_{OP} decreases slightly during the chewing period before swallowing due to dissolution phenomenon (figure 3.a). Then, it decreases sharply at the moment of swallowing. After that, only a small product portion remains in the mouth. The

main phenomenon responsible for product volume variations appears to be the swallowing event, the dissolution having only a minor contribution. The change in saliva volume in mouth V_{OS} is dependent on the rate of saliva incorporation in the liquid phase of the bolus Q_{OS} (assumed constant) (figure 3.b). Therefore, the longer the chewing period before swallowing, the larger this volume is. Each swallow brings the volume of saliva in the mouth down to the baseline. The volume of product dissolved in the liquid phase of the bolus V_{OPD} (figure 3.c) has a minor contribution in the total volume of the liquid phase of the bolus V_{OL}, compared to the volume of incorporated saliva V_{OS}.

The contact area between the solid and liquid phases of the bolus in the mouth A_{OLP} increases rapidly before the first swallow because of product fragmentation during the chewing process (figure 3.d). Then, the contact area decreases sharply at swallowing. Its variation between secondary swallows is small, because of the small amount of product remaining in the mouth.

The concentration of aroma compounds in the air in the oral cavity C_{OA} increases until swallowing due to mass transfer from the liquid bolus to the air (figure 3.e). The velopharynx opening causes small cyclical depressions. Then, swallowing creates a renewal of air and therefore a sharp decrease in concentration. Before the first swallowing, the concentration of aroma compound in the liquid phase of the bolus C_{OL} increases due to the supply of aroma compounds from product (figure 3.f). This increase is promoted by a large contact area between the solid product and the liquid bolus. After swallowing, little product remains in the mouth; the transfer of aroma compound to the air and saliva dilution become dominant, which explain the overall decrease in aroma compound concentration in the liquid phase of the bolus. Globally, the change in concentration of aroma compounds in the air in the oral cavity C_{OA} follows the concentration in the liquid phase of the bolus C_{OL}. The concentration of aroma compounds in the pharyngeal deposit C_{FL} is null during the consumption stage preceding the first swallow (figure 3.g). After swallowing, a portion of the liquid fraction of

449 the bolus is deposited in the pharynx, which causes a sharp increase in the concentration.
450 Then, aroma compounds in the pharyngeal deposit are gradually released to the air phase.
451 During secondary swallowing events, the deposit is renewed by the food bolus coming from
452 the oral cavity. However, the new layer is already depleted in aroma compounds, which leads
453 to a general decrease in C_{FL}. The air in the pharynx (C_{FA}) receives aroma compounds from
454 the pharyngeal deposit and from the air of the oral cavity at each velopharynx opening (minor
455 peaks observed on the curve) (figure 3.h). Overall, the kinetics of concentration in the
456 pharynx C_{FA} follow the one in oral cavity C_{OA}, up to a dilution factor. The concentration of
457 aroma compounds in the air in the nasal cavity C_{NA} evolves similarly to the one of the air in
458 the pharynx C_{FA} (figure 3.i). However, each inspiration of fresh air, which is aroma-free,
459 makes the signal of the concentration in the nasal cavity C_{NA} decrease to zero.
460 As illustrated in figure 3, modelling provided insight in the change in non measured variables.
461 An important outcome was an improved understanding of mechanisms governing aroma
462 release kinetics and of the underlying assumptions.

463 4.2.Comparison of model predictions with experimental data for ethyl propanoate

464 As no interaction with lubricated mucosa was assumed for ethyl propanoate, simulations were
465 performed using the model without lubricated mucosa compartment. To compare model
466 simulations with experimental *in vivo* release data for ethyl propanoate, the air flow rate
467 resulting from the frequency of velopharynx opening was adjusted to fit the simulated release
468 kinetics before the first swallowing. The rate of saliva incorporation into the food bolus was
469 also adjusted so that the simulated release kinetics after the first deglutition fitted the decay
470 phase of the experimental curve.
471 All simulations have been satisfactorily fitted to experimental data (the average error of the
472 model, for all cheeses and all individuals, was only 5.88%±2.81). The two unknown

parameters of the model (the average rate of saliva incorporation into the bolus and the frequency of velopharyngeal opening) could be estimated.

Figure 4 presents some comparisons of simulations and experimental data for panelists S001 and S101. We can observe that these two individuals present diversified consumption and aroma release behaviours: for example, panellist S001 exhibits a consistently longer mastication time before the first swallow than panellist S101, and both panellists have longer mastication times for firm matrices, as one could expect. In spite of this diversity, the model correctly described the *in vivo* release profiles. Some slight deviations can be noticed, as for instance on figures 4.a and 4.b at about 10s and 30s respectively. A possible explanation could be that individuals have more complex behaviour during food consumption than currently assumed in the model; for example, the amplitude of jaw movement related to parameter ΔV_{OA} in Eq. 5 may vary in the course of the mastication process. This cannot be correctly represented by the model with constant values of physiological parameters. One should also bear in mind that panellists' behaviour is not fully reproducible and the greyed area in Figure 4 represents an interval of ±1 standard deviation of 3 replicate experiments, which is statistically expected to contain less than 58% of the data.

The mean rate of saliva incorporation into the bolus Q_{OS} (for all cheeses and all panelists), experimentally determined using the percentage of saliva incorporated in the bolus and the average chewing time, is 7.88±4.39 mL/min (figure 5, bar B). Its value remains similar to the one of Q_{OS} estimated by fitting simulations to experimental data (9.00 ± 3.65 mL/min, bar C in figure 5). These values are also comparable (mean and standard deviation) to the salivary flow values measured experimentally during food consumption by other authors [28-30].

Overall, the average rate of saliva incorporation into the bolus, either measured directly or estimated by fitting simulations to experimental data, was statistically much higher than the salivary flow measured with mechanical stimulation (9.00±3.65 mL/min *vs.* 2.65±0.87

mL/min, bar A in Figure 5) as already observed by Gaviao *et al*. [25] (7.82±4.53 mL/min *vs*. 1.40±0.67 mL/min), meaning that the salivary flow obtained with a mechanical stimulus is not representative of the actual one during product consumption.

When products are compared (table 1), it appears that the average rate of saliva incorporation into the bolus for the cheese matrix Fh (firm with a high-fat content) is statistically lower than for the others cheese matrices (2-fold factor between cheese matrix Fh and cheese matrices Sh and FFl), probably due to a longest consumption duration of cheese matrix Fh, as already observed in previous studies [23]. Indeed, the rate of incorporation of saliva into the bolus can be expressed as: $Q_{OS} = \frac{initial\ volume\ of\ saliva}{duration\ of\ consumption\ before\ swallowing} + salivary\ flow\ rate$, with the initial volume of saliva in mouth being the same whatever the consumption duration. If we assume that the salivary flow rate is constant during time, it follows that the longer the consumption duration, the smaller Q_{OS} will be. The presence of fat can also induce a decrease in salivary flow, as already observed during the consumption of model cheese matrices [31]. In the present study, it is likely that the low value of the average rate of saliva incorporation into the bolus for the cheese matrix Fh is the result of the two phenomena mentioned above.

4.3. Comparison of model predictions with experimental data for 2-nonanone

In vivo observations highlighted that ethyl propanoate and 2-nonanone exhibit quite different behavior in terms of persistence (figure 6): the release amount for 2-nonanone during phase 2 was systematically higher for all individuals and all cheese matrices than for ethyl propanaote (significant difference between the areas under curve of the two aroma compounds, Friedman and Bonferroni tests, $p<0.05$, not shown). We assumed that this phenomenon was the result of an interaction between this molecule and lubricated mucosa. A specific experiment, based on swallowing of aromatized air, was performed to check this assumption (see Material and Method section). An example of standardized release curve is shown in figure 7 for one panelist. Statistical analysis confirmed that 2-nonanone (solid line) persists much longer than

ethyl propanoate (dotted line) in the exhaled air. This was observed for all panelists and all replicates. Measurements by PTR-MS of the *in vitro* release of these two molecules by diluting the headspace of a vial containing the same aqueous flavoured solution excluded a retention effect of the PTR-MS transfer line. All these results confirmed the existence of a significant retention of the 2-nonanone by oral, pharyngeal and/or nasal lubricated mucosa. This phenomenon has already been highlighted for other volatile compounds such as ethanol or menthol [4, 32].

Simulations performed with the model including lubricated mucosa compartments were compared to *in vivo* release data for 2-nonanone for cheese matrices FFl and Sl. No data was available for the two others cheese matrices since 2-nonanone was not detected because of its high hydrophobicity and of retention by fat. The frequency of velopharynx opening and the rate of saliva incorporation into the food bolus which were previously found for ethyl propanoate were kept identical. Results showed that all simulations satisfactorily fitted experimental data if a mucosa layer thickness of 100 µm and a transfer coefficient of 1×10^{-1}cm/s were fixed for all individuals (figure 8). The average error of the model was 13.16%±6.80, for the two cheese matrices tested and for the ten individuals. These results will have to be refined in the future, through dedicated experiments to measure aroma compound retention by lubricated mucosa.

4.4. Velopharynx opening

The results of the model fitting suggested that velopharynx opening can be different between individuals. We found that in 53% of cases, the velopharynx opening was synchronized with chewing frequency; in 37% of cases, it was synchronized with respiratory frequency and in the 10% remaining cases, subjects had an intermediate behavior. Although little data is available on this topic in the literature, these results are consistent with observations from Matsuo *et al*. [18], who studied the velopharynx opening of 9 persons by videofluorography

548 during the consumption of various foods (banana, cookie, meat). They found that the opening
549 frequency varied widely among subjects, but that the opening time was related to jaw
550 movements. A link between breathing and velopharynx movements was also highlighted.

551 4.5. Analysis of model sensitivity

552 An analysis of model sensitivity was performed to evaluate the effect of some physiological
553 or physicochemical parameters on the variation of nasal concentration with time. A standard
554 nasal concentration curve was determined using mean values for panellist characteristics.
555 Then, each parameter was multiplied or divided by a factor of two (which is representative of
556 the typical variability of physiological parameters).

557 To assess the effect of each parameter on release intensity, each simulated kinetic was scaled
558 by the maximum of the standard nasal concentration curve. Three parameters were found to
559 have a strong positive effect on release intensity: the product dissolution rate in the mouth, the
560 mass transfer coefficient of aroma compound in the bolus and the air-bolus contact area in the
561 mouth. The respiratory frequency had a significant negative effect on nasal aroma
562 concentration by increasing aroma compound removal.

563 To assess the effect of each parameter on release dynamics, independently from global
564 intensity, each simulated kinetic was scaled by its own maximum intensity. Results showed
565 that only three out of the twenty parameters of the model had a major influence on the overall
566 kinetics (results not shown): the rate of saliva incorporation into the bolus during food
567 consumption Q_{OS}, the duration of the mastication before the first swallowing and the
568 velopharynx opening (amplitude ΔV_{OA} and frequency $fr_{opening}$). For example, an increase in
569 the rate of saliva incorporation into the bolus during food consumption resulted in a decrease
570 in the nasal concentration after the first swallow, due to the renewal of liquid phases present
571 in the mouth and pharynx (supply of fresh saliva). These results from sensitivity analysis and
572 the high level of uncertainty and of variability among individuals for physiological parameters

explained why the rate of saliva incorporation into the bolus during food consumption Q_{OS} and the frequency of the velopharynx opening $fr_{opening}$ were selected as the two degrees of freedom of the model.

5. Conclusions

In conclusion, it appears that the proposed model adequately simulated ethyl propanoate release during the consumption of masticated matrices by a panel of ten individuals. The estimation of the average rate of saliva incorporation into the bolus and the frequency of velopharyngeal opening were in agreement with literature data. This study pointed out the role of mastication on the release of aroma compounds during consumption of solid food, by notably impacting the residence time of products in mouth and the opening of velopharynx during product intra-oral manipulation, which ensures a continuous supply of aroma compounds in the nose. Model sensitivity analysis highlighted that the parameters having a major impact on flavour release when eating a solid food product are partly different from the ones highlighted in the case of liquid or semi-liquid food [7]: in that case, the mass transfer coefficient in the bolus, the breath flow rate and the thickness of post-deglutition pharyngeal residue were the three key factors governing the release of aroma compounds. Differences with previous work on liquid and semi-liquid food products mainly come from the duration of food residence in the mouth.

The release of 2-nonanone highlighted the existence of retention phenomenon of this molecule by lubricated mucosa. The model successfully accounted for this phenomenon. Further work could help clarifying the binding mechanisms and come up with a satisfactory quantitative description of the retention phenomenon [33, 34].

Overall, experimental release studies combined with mechanistic modelling help gaining new insight into the complex phenomena of *in vivo* aroma compound release during the

consumption of a solid food, by understanding the relative contributions of product properties, of individual characteristics and of their interactions.

Nomenclature

Symbol	Unit	Parameter
A	cm^2	Product/saliva contact area
A_{FAL}	cm^2	Air/liquid bolus contact area in the pharynx
A_{OAL}	cm^2	Air/ liquid bolus contact area in the oral cavity
A_{NAM}	cm^2	Air/lubricated mucosa contact area in the nasal cavity
A_{OLP}	cm^2	Liquid bolus/product contact area in the oral cavity
C_{FA}	g/cm^3	Aroma concentration in the air in the pharynx
C_{FL}	g/cm^3	Aroma concentration in the liquid bolus in the pharynx
C^*_{FL}	g/cm^3	Aroma concentration at the air/liquid bolus interface in the pharynx
C_{NA}	g/cm^3	Aroma concentration in the air in the nasal cavity
C_{NM}	g/cm^3	Aroma concentration in the lubricated mucosa in the nasal cavity
C_{OA}	g/cm^3	Aroma concentration in the air in the oral cavity
C^*_{OAL}	g/cm^3	Aroma concentration at the air/ liquid bolus interface in the oral cavity
C_{OL}	g/cm^3	Aroma concentration in the liquid bolus in the oral cavity
C_{OP}	g/cm^3	Aroma concentration in the product in the oral cavity
C_{P_salt}	g/cm^3	Salt concentration in the solid product
C_{S_salt}	g/cm^3	Salt concentration in artificial saliva
C_{TA}	g/cm^3	Aroma concentration in the trachea
E	cm	Residual bolus layer thickness in the pharynx
e_{NM}	cm	Layer thickness of the lubricated mucosa in the nasal cavity
F_R	Number of cycles/s	Respiratory frequency
$fr_{masticatory}$	Number of chews/s	Masticatory frequency
$fr_{opening}$	Occurrence number/s	Opening frequency of the velopharynx
HM_{bolus}	%	Moisture content of the bolus
HM_{cheese}	%	Moisture content of cheese product
K_{FAL}		Air/ liquid bolus partition coefficient in the pharynx

K_{NAM}		Air/ mucosa partition coefficient in the nasal cavity
K_{OAL}		Air/ liquid bolus partition coefficient in the oral cavity
k_{FL}	m/s	Mass transfer coefficient in the liquid bolus in the oral pharynx
k_{NM}	m/s	Mass transfer coefficient in the lubricated mucosa in the nasal cavity
k_{OA}	m/s	Mass transfer coefficient in the air phase in the oral cavity
k_{OL}	m/s	Mass transfer coefficient in the liquid bolus in the oral cavity
R	m	Average radius of particles in the bolus.
r_L	g/g	Mass fraction of liquid bolus remaining in the mouth after deglutition
r_{cs}	g/g	Cheese/saliva mass ratio
t_{deg}	s	Swallowing moment
Q_{NA}	cm^3/s	Air flow rate coming from the nasal cavity
Q_{OA}	cm^3/s	Air flow rate coming from the oral cavity
Q_{OS}	cm^3/s	Average rate of saliva incorporation in the bolus
Q_{TA}	cm^3/s	Air flow rate coming from the trachea
v	cm/s	Product dissolution rate in the saliva
V_{FA}	cm^3	Volume of air in the pharynx
V_{FL}	cm^3	Volume of liquid bolus in the pharynx
V_{lung}	cm^3	Lung volume
V_{NA}	cm^3	Volume of air in the nasal cavity
V_{NM}	cm^3	Volume of lubricated mucosa in the nasal cavity
V_{OA}	cm^3	Volume of air in the oral cavity
ΔV_{OA}	cm^3	Amplitude of mouth volume variation during mastication
V_{OL}	cm^3	Volume of liquid bolus in the oral cavity
V_{OP}	cm^3	Volume of product in the oral cavity
V_{OPD}	cm^3	Volume of dissolved product in the bolus of the oral cavity
V_{OS}	cm^3	Volume of saliva in the bolus

$V_{Salivadeg+}$	cm^3	Volume of saliva usually present in the oral cavity after swallowing
V_T	cm^3	Tidal volume
ϕ_{FAL}	g/s	Volatile mass flux between the air and the liquid bolus in the pharynx
ϕ_{NAM}	g/s	Volatile mass flux between the air and lubricated mucosa in the nasal cavity
ϕ_{OAL}	g/s	Volatile mass flux between the air and the liquid bolus in the oral cavity
ϕ_{salt}	g/s	Salt mass flux between the product and saliva
τ	s	Characteristic time of the aroma release decay

Remark: The solid part of the bolus consists of the non-dissolved part of the food product.

Acknowledgements

The authors gratefully acknowledge the French National Research Agency (ANR) project "SensInMouth" for financial support.

References

[1] Chen, J. S. Food oral processing - a review. *Food Hydrocolloids*, **2009**, 23(1), 1-25.

[2] Harrison, M., B. P. Hills, J. Bakker and T. Clothier. Mathematical models of flavor release from liquid emulsions. *Journal of Food Science*, **1997**, 62(4), 653-664.

[3] Overbosch, P., W. G. M. Afterof and P. G. M. Haring. Flavor release in the mouth. *Food Review International*, **1991**, 7, 137.

[4] Normand, V., S. Avison and A. Parker. Modeling the Kinetics of Flavour Release during Drinking. *Chemical. Senses*, **2004**, 29(3), 235-245.

[5] Wright, K. M. and B. P. Hills. Modelling flavour release from a chewed bolus in the mouth: Part II. The release kinetics. *International journal of Food Science and Technology*, **2003**, 38(3), 361-368.

[6] Tréléa, I. C., S. Atlan, I. Déléris, A. Saint-Eve, M. Marin and I. Souchon. Mechanistic mathematical model for in vivo aroma release during eating of semi-liquid foods. *Chemical Senses*, **2008**, 33(2), 181-192.

[7] Doyennette, M., C. De Loubens, I. Déléris, I. Souchon and I. C. Tréléa. Mechanisms explaining the role of viscosity and post-deglutitive pharyngeal residue on in vivo aroma release: A combined experimental and modeling study *Food Chemistry*, **2011**, 128(2), 380-390.

[8] Harrison, M., S. Campbell and B. P. Hills. Computer simulation of flavor release from solid foods in the mouth. *Journal of Agricultural and Food Chemistry*, **1998**, 46(7), 2736-2743.

[9] de Roos, K. B. and K. Wolswinkel. *Non-equilibrium partition model for predicting flavour release in the mouth*. Elsevier Science, **1994**.

[10] Hills, B. P. and M. Harrison. Two-film theory of flavour release from solids. *International journal of Food Science and Technology*, **1995**, 30, 425-436.

[11] Peyron, M. A., A. Mishellany and A. Woda. Particle Size Distribution of Food Boluses after Mastication of Six Natural Foods. . *Journal of Dental Research*, **2004**, 83(7), 578-582.

[12] Tobitsuka, K., M. Miura and S. Kobayashi. Retention of a European Pear Aroma Model Mixture Using Different Types of Saccharides. *Journal of Agricultural and Food Chemistry*, **2006**, 54, 5069-5076.

[13] Agrawal, K. R., P. W. Lucas, J. F. Prinz and I. C. Bruce. Mechanical properties of foods responsible for resisting food breakdown in the human mouth. *Archives of Oral Biology*, **1997**, 42(1), 1-9.

[14] van der Bilt, A., L. W. Olthoff, H. W. van der Glas, K. van der Weelen and F. Bosman. A mathematical description of the comminution of food during mastication in man. *Archives of Oral Biology*, **1987**, 32(8), 579-586.

[15] Wright, K. M. and B. P. Hills. Modelling flavour release from a chewed bolus in the mouth: Part I. Mastication. *International Journal of Food Science and Technology*, **2003**, 38(3), 351-360.

[16] de Loubens, C., M. Panouillé, A. Saint-Eve, I. Déléris, I. C. Tréléa and Souchon I. . Mechanistic model of in vitro salt release from model dairy gels based on standardized breakdown test simulating mastication. *Journal of Food Engineering* **2011**, 105(1), 161-168.

[17] Cussler, E. L. *Diffusion. Mass Transfer in Fluid Systems.* University Press, Cambridge, **1997**.

[18] Matsuo, K., H. Metani, K. A. Mays and J. B. Palmer. Effects of Respiration on Soft Palate Movement in Feeding. *Journal of Dental Research*, **2010**, 89, 1401-1406.

[19] Doyennette, M., I. Déléris, A. Saint-Eve, A. Gasiglia, I. Souchon and I. C. Tréléa. The dynamics of aroma compound transfer properties in cheeses during simulated eating conditions. *Food Research International*, **2011**, 44(10), 3174-3181.

[20] Levitzky, M. G. *Pulmonary physiology*, **2003**.

[21] Hornung, D. E., S. L. Youngentob and M. M. Mozell. Olfactory Mucosa-Air Partitioning of Odorants. *Brain Research Bulletin.*, **1987**, 413(1), 147-154.

[22] Shojaei, A. H. Buccal mucosa as a route for systemic drug delivery: a review. *Journal of Pharmaceutical Sciences*, **1998**, 1(1), 15-30.

[23] Repoux, M., H. Laboure, P. Courcoux, I. Andriot, E. Semon, C. Yven, G. Feron and E. Guichard. Combined effect of cheese characteristics and food oral processing on in vivo aroma release. *Flavor and Fragrance Journal*, **2012**, 27(6), 414-423.

[24] Watanabe, S. and C. Dawes. A Comparison of the Effects of Tasting and Chewing Foods On the Flow-rate of Whole Saliva In Man. *Archives of Oral Biology*, **1988**, 33, 761-764.

[25] Gaviao, M. B., L. Engelen and A. Van der Bilt. Chewing behavior and salivary secretion. *European Journal of oral science*, **2004**, 112(1), 19-24.

[26] Yven, C., J. Patarin, A. Magnin, H. Labouré, M. Repoux, E. Guichard and G. Féron. Consequences of individuals chewing strategies on bolus rheological properties at the swalllowing treshold. *Jourrnal of Texture Studies*, **2012**, 43(4), 309-318.

[27] Ettre, L. S., C. Welter and B. Kolb. Determination of gas-liquid partition coefficients by automatic equilibrium headspace-gas chromatography utilizing the phase ratio variation method. *Chromatographia*, **1993**, 35(1/2), 73-84.

[28] Mioche, L., O. Bourdiol, S. Monier and J. F. Martin. The relationship between chewing activity and food bolus properties obtained from different meat textures. *Biosciences, Biotechnology, Biochemistry*, **2002**, 69(9), 1669-1676.

[29] Patarin, J., D. Blésès, A. Magnin, C. Yven, H. Labouré and G. Féron. Mechanical characterization of cheese food bolus: a new device. *Food Oral Processing congress*, Leeds, U.K., **2010**.

[30] Anderson, K., G. S. Throckmorton, P. H. Buschang and H. Hayasaki. The effects of bolus hardness on masticatory kinematics. *Journal of Oral Rehabilitation*, **2002**, 29(7), 689-696.

[31] Tarrega, A., C. Yven, E. Sémon and C. Salles. Aroma release and chewing activity during eating different model cheeses. *International Dairy Journal*, **2008**, 18(8), 849-857.

[32] Van Ruth, S. M., J. Frasnelli and I. Carbonell. Volatile flavour retention in food technology and during consumption: Juice and custard examples. *Food Chemistry*, **2008**, 106(4), 1385-1392.

[33] Medinsky, A. and J. A. Bond. Sites and mechanisms for uptake of gases and vapors in the respiratory tract. *Toxicology*, **2001**, 160, 165-172.

[34] Kurtz, D. B., K. Zhao, D. E. Hornung and P. Scherer. Experimental and numerical determination of odorant solubility in nasal and olfactory mucosa. *Chemical Senses*, **2004**, 29(9), 763-773.

[35] Salles, C., M. C. Chagnon, G. Féron, E. Guichard, H. Labouré, M. Morzel, E. Sémon, A. Tarrega and C. Yven. In-mouth mechanisms leading to flavor release and perception. *Critical Reviews in Food Science and Nutrition*, **2011**.

Figure captions

Figure 1. Schematic representation of the chronological steps of the consumption of a solid food product.

Figure 2. Schematic representation of the interconnected compartments and of the mechanisms involved in flavour release during the consumption of a solid food product.

Figure 3. Time variation of 9 model variables for the release of aroma compounds during the consumption of a solid product: (a) solid product volume in the mouth V_{OP}, (b) volume of saliva in the mouth V_{OS}, (c) volume of dissolved product in the liquid phase of the bolus V_{OPD}, (d) contact area between solid and liquid phases of the bolus in the mouth A_{OLP}, (e) aroma compound concentration in the air of the oral cavity C_{OA}, (f) aroma compound concentration in the liquid phase of the bolus in the mouth C_{OL}, (g) aroma compound concentration in the pharyngeal deposit C_{FL}, (h) aroma compound concentration in the air in the pharynx C_{FA} and (i) aroma compound concentration in the air in the nasal cavity C_{NA}. Case of the consumption of the cheese matrix FFl and for ethyl propanoate, with typical values of the physiological parameters. Time 0 corresponds to the moment of the first swallowing. Vertical lines indicate the time of product introduction in mouth and the successive swallowing events.

Figure 4. Comparison of simulated and experimental release profiles for ethyl propanoate for panelists S001 (a-d) and S101 (e-h) and for cheese matrices FFl (a, e), Fh (b, f), Sl (c, g) and Sh (d, h). For each figure, the simulation is represented by a thick line, the average curve of the three replicates by a thin line and the envelope curve representing the standard deviation of three repetitions by the "gray" area. The characteristic moments of consumption (product introduction in mouth and the successive swallowing events) are represented by vertical lines. The two graphs in the form of bars at the right of the main figure present the values of two parameters before and after model fitting. The initial value is symbolized by a square and the

724 estimated value after the adjustment of the model by a triangle. The extreme values
725 (maximum and minimum) give the physiological range of variation for each parameter
726 (extracted from the initial panel of 50 individuals).
727 Figure 5. Comparison of the average rate of saliva incorporation into the bolus estimated by
728 model fitting with literature data. A) Salivary flow rate (parafilm stimulation), B) Average
729 rate of saliva incorporation in the bolus (determined experimentally by measuring the dry
730 extract of the bolus), C) Average rate of saliva incorporation in the bolus (estimated by model
731 fitting), D) Average rate of saliva incorporation in the bolus given by [25]), E) Average rate
732 of saliva incorporation in the bolus reported in [35]) and F) Average rate of saliva
733 incorporation in the bolus reported in [24]).
734 Figure 6. Comparison of *in vivo* release profiles of ethyl propanoate (thin envelope curve and
735 dark gray line) and 2-nonanone (thin envelope curve and light gray line) for subject S001,
736 cheese matrix FFl. The characteristic moments of consumption (product introduction in
737 mouth and the successive swallowing events) are represented by vertical lines.
738 Figure 7. Comparison of *in vivo* release of ethyl propanoate (dotted line) and 2-nonanone
739 (solid line) following the ingestion of flavoured air (1 panelist, 1 replicate). The data are
740 normalized to their maximum intensity.
741 Figure 8. Comparison of simulated and experimental release profiles for 2-nonanone for
742 panelist S001 for cheese matrices (a) FFl and (b) Sl, and for panelist S101 for cheese matrices
743 (c) FFl and (d) Sl. For each figure, simulation is represented by a thick line, the average curve
744 on the three replicates by a thin line and the envelope curve representing the standard
745 deviation of three repetitions by the "gray" area. The characteristic moments of consumption
746 (product introduction in mouth and successive swallowing events) are represented by vertical
747 lines.
748

Table captions

Table 1. Comparison of the average rates of saliva incorporation into the bolus (in mL/min) for the 4 cheese matrices. The letters indicate the classification group of the products (Friedman and Bonferroni tests are significant at the level 5%).

4. Figure1

Click here to download 4. Figure: Figure 1_doyennette.pdf

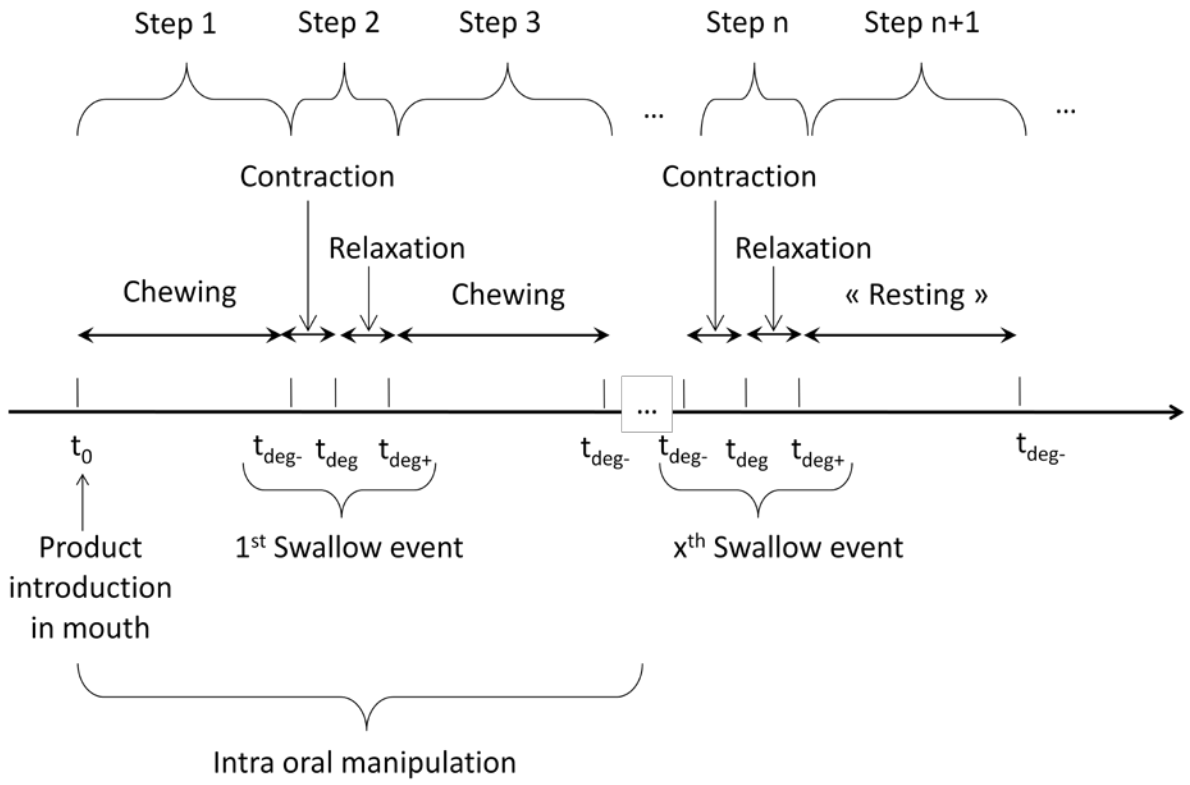

Figure 1.

4. Figure2

Click here to download 4. Figure: Figure 2_doyennette.pdf

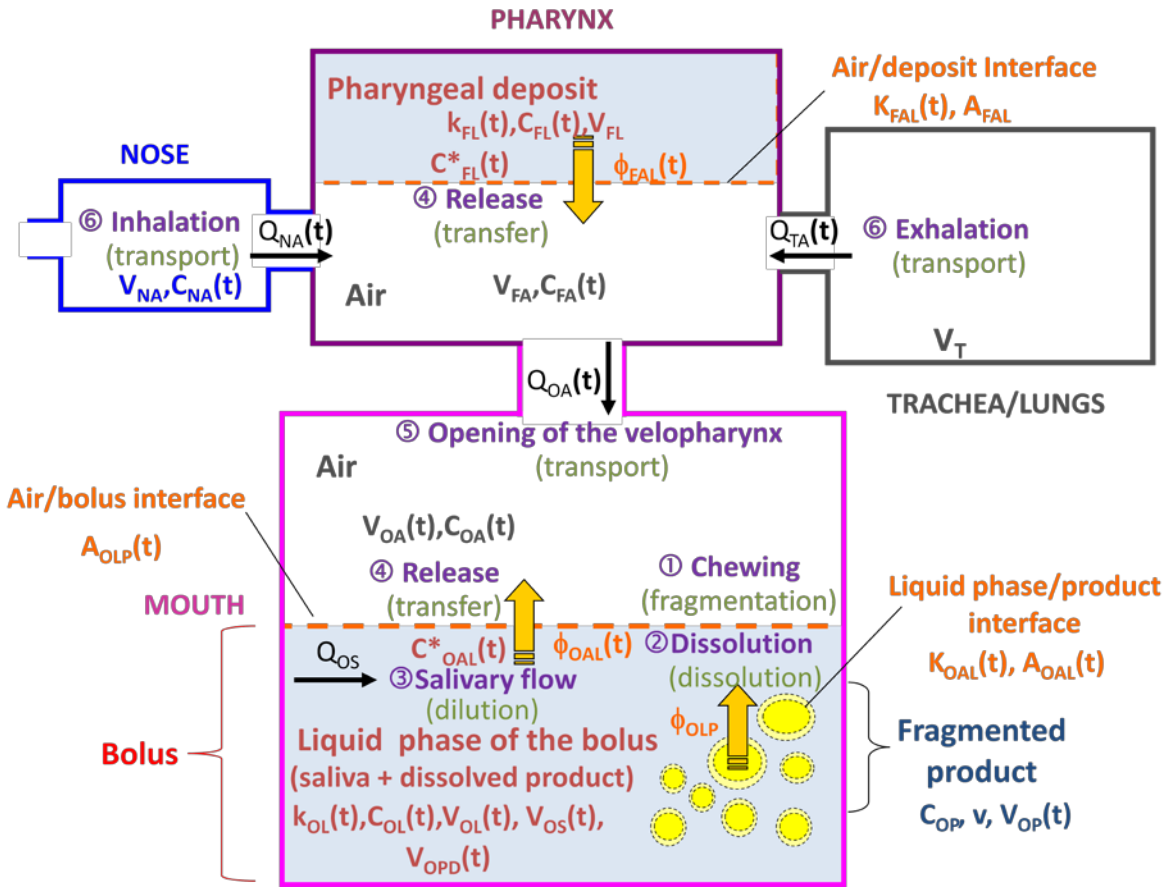

Figure 2.

4. Figure3

Click here to download 4. Figure: Figure 3_doyennette.pdf

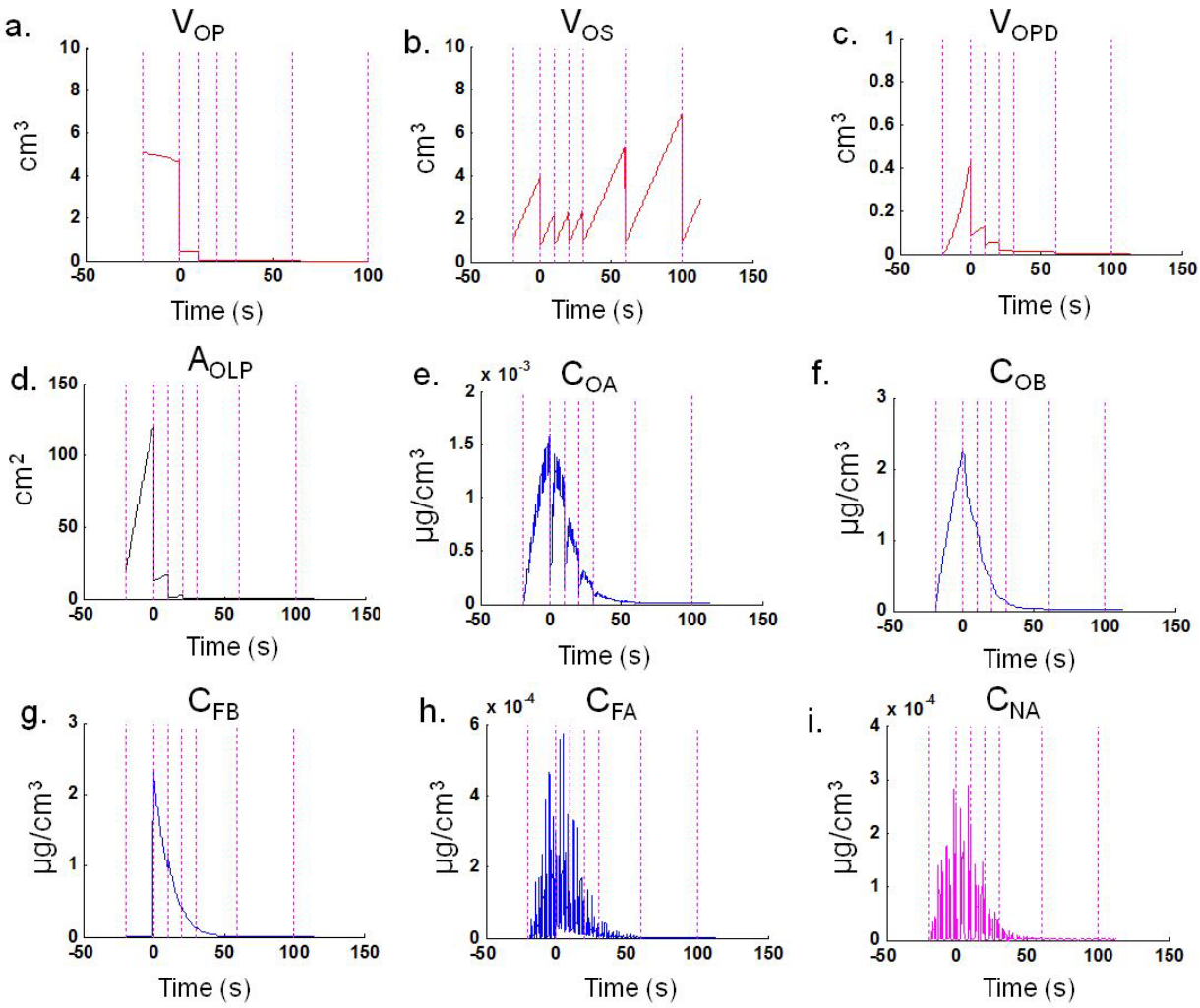

Figure 3.

4. Figure4

Click here to download 4. Figure: Figure 4_doyennette.pdf

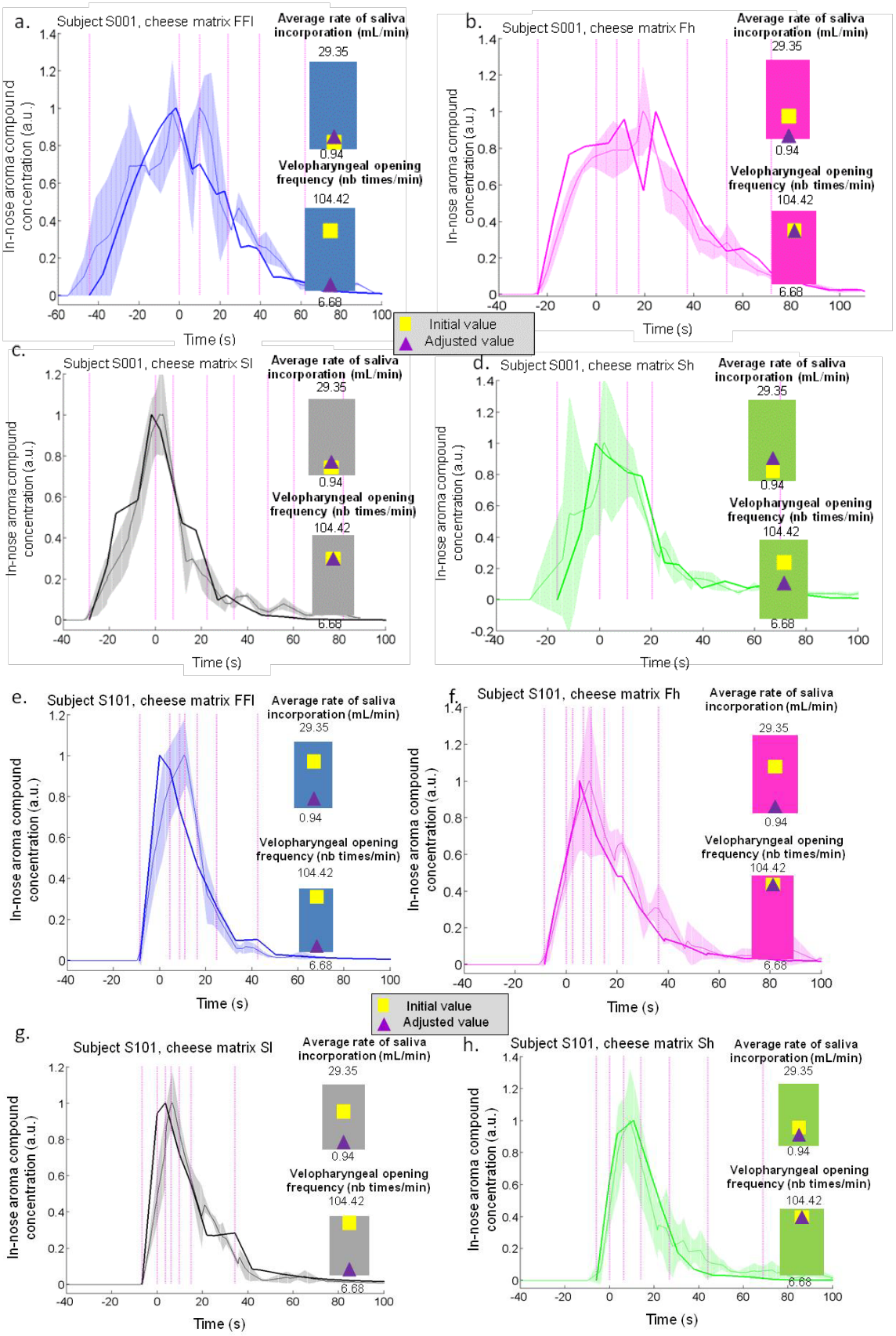

Figure 4.

4. Figure5

Click here to download 4. Figure: Figure 5_doyennette.pdf

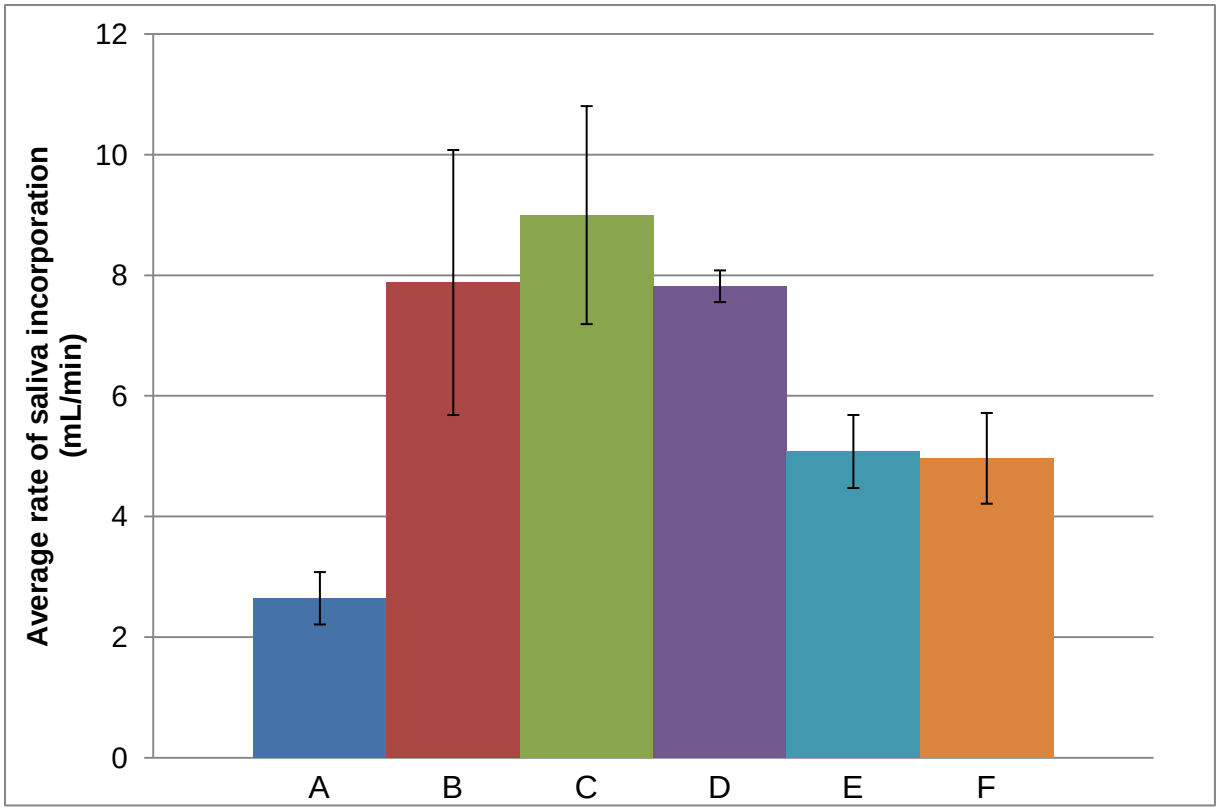

Figure 5.

4. Figure6

Click here to download 4. Figure: Figure 6_doyennette.pdf

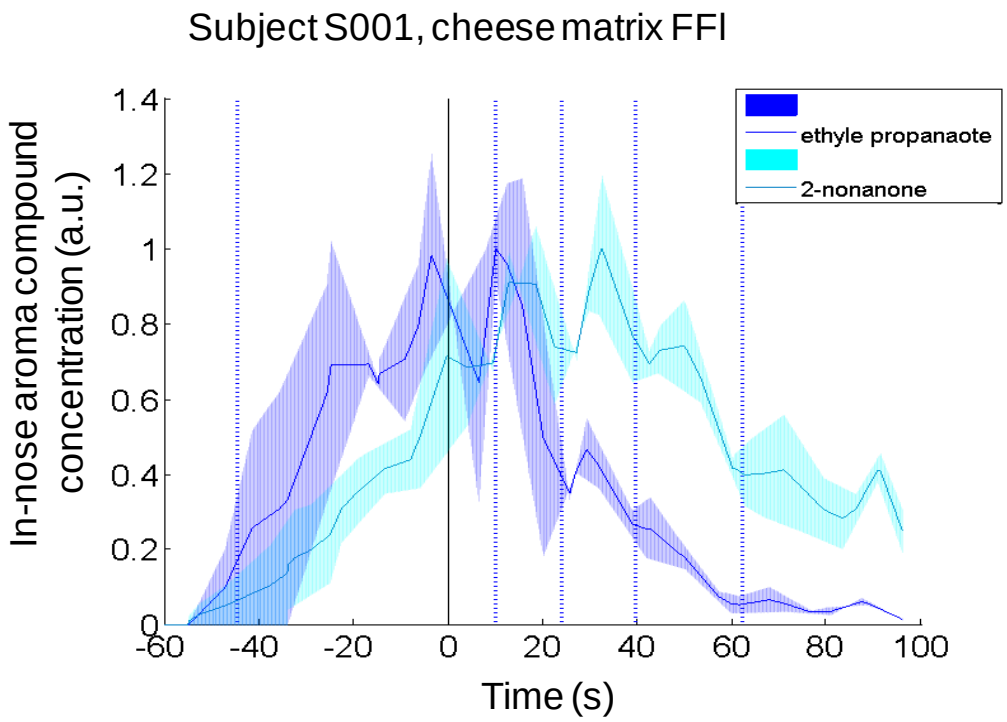

Figure 6.

4. Figure7

Click here to download 4. Figure: Figure 7_doyennette.pdf

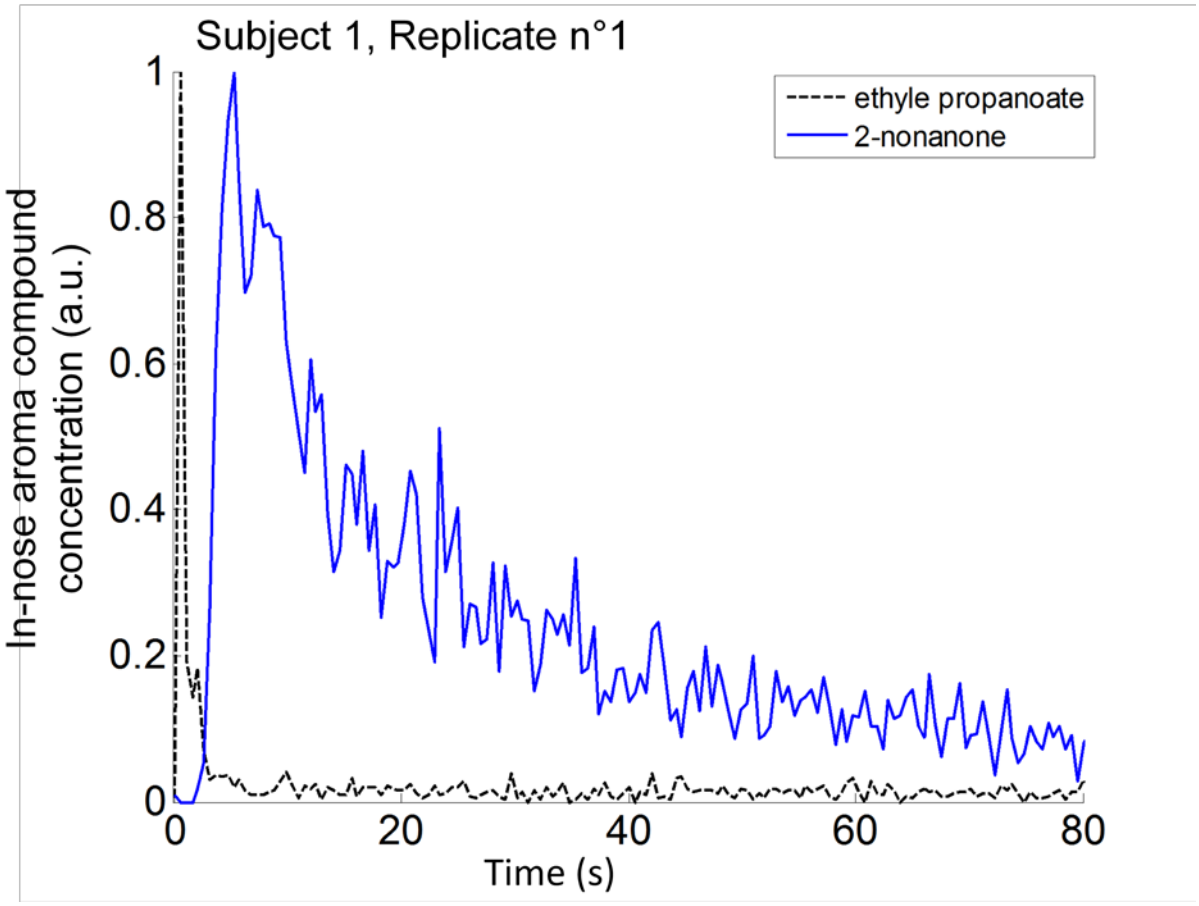

Figure 7

4. Figure8

Click here to download 4. Figure: Figure 8_doyennette.pdf

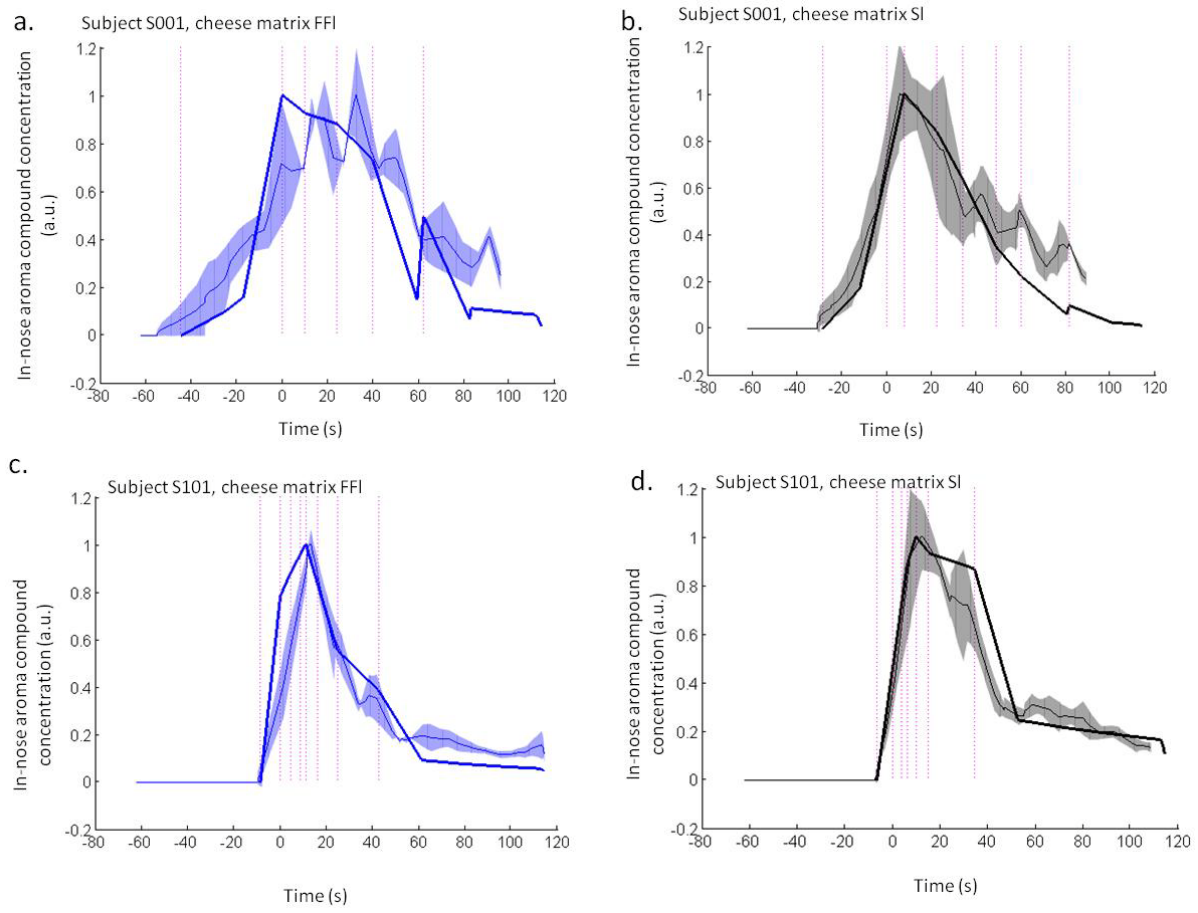

Figure 8

5. Table1

Table 1.

Rate of saliva incorporation	FFl	Sh	Sl	Fh
Mean value (mL/min)	10.50	10.80	9.43	5.27
Standard deviation (mL/min)	5.70	4.97	6.16	8.08
Group	A	A	AB	B